

# Locality of correlation in density functional theory

Kieron Burke,<sup>1</sup> Antonio Cancio,<sup>2</sup> Tim Gould,<sup>3</sup> and Stefano Pittalis<sup>4</sup>

<sup>1</sup>*Department of Chemistry, University of California, Irvine, CA 92697*

<sup>2</sup>*Department of Physics and Astronomy, Ball State University, Muncie, IN 47306*

<sup>3</sup>*Qld Micro- and Nanotechnology Centre, Griffith University, Nathan, Qld 4111, Australia*

<sup>4</sup>*CNR-Istituto di Nanoscienze, Via Campi 213A, I-41125 Modena, Italy*

(Dated: December 3, 2024)

The Hohenberg-Kohn density functional was long ago shown to reduce to the Thomas-Fermi approximation in the non-relativistic semiclassical (or large- $Z$ ) limit for all matter, i.e, the kinetic energy becomes local. Exchange also becomes local in this limit. Numerical data on the correlation energy of atoms supports the conjecture that this is also true for correlation, but much less relevant to atoms. We illustrate how expansions around large particle number are equivalent to local density approximations and their strong relevance to density functional approximations. Analyzing highly accurate atomic correlation energies, we show that  $E_C \rightarrow -A_C Z \ln Z + B_C Z$  as  $Z \rightarrow \infty$ , where  $Z$  is the atomic number,  $A_C$  is known, and we estimate  $B_C$  to be about 37 millihartrees. The local density approximation yields  $A_C$  exactly, but a very incorrect value for  $B_C$ , showing that the local approximation is less relevant for correlation alone. This limit is a benchmark for the non-empirical construction of density functional approximations. We conjecture that, beyond atoms, the leading correction to the local density approximation in the large- $Z$  limit generally takes this form, but with  $B_C$  a functional of the TF density for the system. The implications for construction of approximate density functionals are discussed.

PACS numbers: 71.15.Mb 31.15.E- 31.15.ve 31.15.xp

## I. INTRODUCTION

Kohn-Sham density functional theory[1] enjoys remarkable popularity, being used in more than 30,000 papers last year[2]. Essentially all these calculations use some approximation to the exchange-correlation energy,  $E_{xc}$ , as a functional of the (spin)-densities[3]. Although many hundreds of such approximations exist and appear in standard codes, most calculations are run with one of a few approximations. These standard approximations [4–8] have been around for almost twenty years and their successes and failures are well-known. Of course there are many excellent improvements beyond these approximations for specific purposes[9, 10].

Although the exact theory of DFT is well-established[11, 12] and rarely questioned these days, it is sometimes claimed that there is no systematic approach to the overall construction of approximate functionals. In fact, this is not true. More than 40 years ago, Lieb and Simon proved that Thomas-Fermi theory become relatively exact for the total (non-relativistic) energy of any system in a limit in which both the particle number  $N$  becomes large and the coordinates are scaled. For atoms, this amounts to  $Z \rightarrow \infty$ , where  $Z$  is the nuclear charge, while keeping the atom neutral ( $Z = N$ ). But the limit also applies to all molecules and solids, once their bond lengths are simultaneously scaled[13]. This limit then implies a systematic approach to the construction of density functionals, by finding density functional corrections to the TF approximation that yield the exact leading corrections to the TF energy. Unfortunately, even in very simple situations, deriving and using these leading corrections can be very demanding, and they will not in

general be explicit density functionals[14–16]. Nonetheless, such functionals are in principle well-defined, if not easily approximated.

The modern world uses the KS variant of DFT, in which only the XC energy needs approximating. Schwinger demonstrated[17, 18] that, for atoms, the local density approximation for exchange becomes relatively exact in the large- $Z$  limit, and a proof (for non-singular potentials) was given by Conlon in the general case[19]. A rigorous proof for atoms was given by Fefferman and Seco[20]. The next correction was estimated by Elliott and Burke[21] and shown to be accurately reproduced by both the B88 functional[4] and the exchange part of PBE[8]. Thus, at the GGA level, the most commonly-used approximations (at least 70% of present calculations[2]) reproduce the leading correction to LDA in this limit. This insight was used (in an inverted piece of logic) to construct the exchange functional in PBEsol[22], which is useful for calculating the equilibrium properties of solids (but not their thermochemistry). The tension between accurate energetics and bond lengths[23, 24] suggests that the GGA form is insufficient to capture all aspects of the leading correction to LDA accurately[22]. The asymptotic expansion for exchange has been used to construct new functional approximations[25–27].

The present paper explores the next logical step in this analysis: Does the correlation energy alone also become relatively exact in LDA in this limit? If so, what is the leading correction, and do standard approximations capture this? These are very fundamental questions about the nature of the XC functional, and our ability to approximate it with semilocal functionals. Such questions

concern properties of the exact functional that are highly relevant to approximations.

We cannot hope to answer this question in general at present, but we can try to answer this question in the one case where we have sufficient data: atoms. By very carefully analyzing accurate correlation energies[28] for a sequence of non-relativistic atoms up to  $Z = 86$ , we find they can be fitted to the following form:

$$E_c \rightarrow -A_c Z \ln Z + B_c Z. \quad (1)$$

The first constant,  $A_c$ , is about 20.7 mHa, and is derived from the uniform electron gas. The second constant,  $B_c$ , is a property of all atoms and is highly *inaccurate* in LDA. We estimate it as 37.1 mHa, whereas in LDA it is -4.5 mHa. However, even this very limited information yields much insight into the nature of the correlation energy functional. At a very elementary level, we see why it has been so much more difficult to identify than the exchange form: The  $1/|\mathbf{r} - \mathbf{r}'|$  behavior of the Coulomb potential produces a  $Z \ln Z$  term, so that only at astronomical values of  $Z$  does the LDA correlation become relatively exact. We find that  $B_c^{\text{LDA}}$  is in fact negative, which is a way of understanding the huge overestimate of LDA correlation energies. We also note that it is *only* the high-density limit of LDA that is relevant to atoms, not the entire density dependence of the uniform gas. Thus, within this analysis, the LDA is only particularly relevant for Coulomb matter in the extreme high-density limit. Of course, for a simple valence metal solid which is well-approximated by a uniform gas, the LDA is needed to produce an accurate correlation energy. Moreover, for energy differences and derivatives with respect to nuclear coordinates that are relevant to bond lengths, more terms in the LDA correlation energy might be relevant.

A first modern attempt to extract the behavior of the correlation energies for large non-relativistic atoms was made by Kunz and Ruedi [29]. They complemented analytical work based on an RPA-like approximation with numerical values from Clementi and Corongiu [30] up to  $Z = 54$ . Their estimate for  $B_c$  is inaccurate, due to inaccuracies in the data and an insufficiently precise extrapolation.<sup>1</sup>

The layout of this article is a little unusual. Almost half the material is introductory, explaining how the Lieb-Simon limit is relevant to approximating density functionals for any component of the energy: Kinetic, exchange, or correlation. This is needed to understand the relevance of the results for correlation. Part of doing this is a simple illustration of how the large- $N$  limit of a series can be used to accurately approximate its value for *all* values of  $N$ , including even  $N = 1$  (or less). We also use

this to give our definition of non-empirical parameters. We next give a substantial amount of background material which also serves to define our notation. The main body of the paper is the careful extrapolation from the results we have for finite  $Z$  to the large- $Z$  limit. We test these extrapolations on cases where we know the answer, and show the results are independent of the details of our procedure. In the final section, we discuss the relevance of our results for density functional approximations.

We use atomic units throughout, so all energies are in Hartrees and all distances in Bohr radii. All calculations employ spin DFT and are entirely non-relativistic.

We beg the forbearance of the reader, as we close with a simple mathematical illustration of the nature and usefulness of expansions as  $N \rightarrow \infty$ , which is the type of expansion we will apply to density functionals. Later, we will tie this particular example to DFT, but for now, consider only the mathematics.

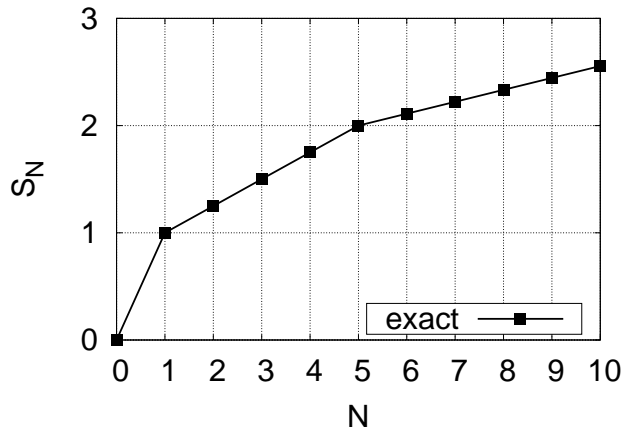


FIG. 1. Partial sum  $S_N$  as a function of  $N$ .

Consider an infinite series with terms:

$$1, 1/4, 1/4, 1/4, 1/4, 1/9, \dots, 1/9, 1/16, \dots, 1/16, 1/25, \dots \quad (2)$$

i.e., a list of  $1/n^2$ , but where each value is repeated  $n^2$  times. If  $f_n$  is the  $n$ -th term in this series, suppose we wish to find the partial sum:

$$S_N = \sum_{n=1}^N f_n. \quad (3)$$

This function is plotted in Fig. 1.

Clearly the sum is unbounded as  $N \rightarrow \infty$ . To expand the series for large  $N$ , consider those values at which  $S$  is an integer:

$$S_{M(j)} = j, \quad (4)$$

where

$$M(j) = \sum_{k=1}^j k^2 = j(j+1)(2j+1)/6. \quad (5)$$

<sup>1</sup> The values reported for  $A_c$  and  $B_c$  on pages 9 and 10 of Ref. [29] appear to have typographical errors. To reproduce Fig. 1, we divide their  $A_c$  by three and reverse the sign of  $B_c$ . But even with these corrections, the resulting value for  $B_c$  is inaccurate.

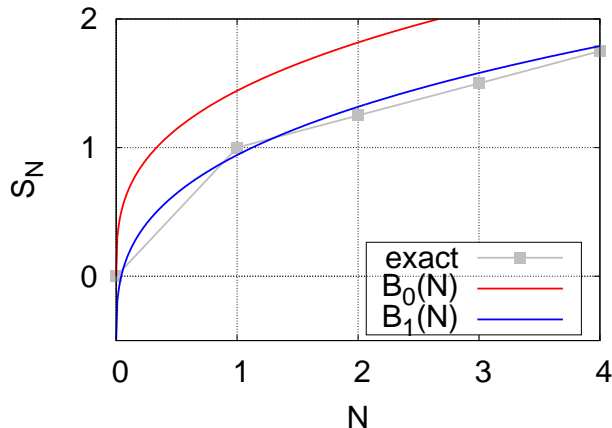


FIG. 2.  $S_N$  and its expansion for large- $N$ , including just the leading term, and adding the first correction.

Expanding  $j(M)$  in inverse powers of  $M^{-1/3}$ , we find

$$j(M) = (3M)^{1/3} - 1/2 - \dots \quad (6)$$

yielding

$$S_N \rightarrow b_0(N) + b_1(N) + b_2(N) + \dots, \quad (7)$$

where  $b_0(N) = (3N)^{1/3}$ ,  $b_1(N) = -1/2$ , etc. We then define the sum up to a given order in  $N^{1/3}$ :

$$B_p(N) = \sum_{k=1}^p b_k(N) \quad (8)$$

and compare these with the exact curve in Fig. 2. The most important point for now is that, including only the first two terms, yields a very reasonable approximation to  $S_N$ , i.e., the large- $N$  expansion can be used to approximate the series for *any* value of  $N$ , all the way down to  $N = 1$ . Thus, even though we might only care about, e.g.,  $N < 100$ , we can find good approximations by studying the approach to the large- $N$  limit. We will return to this example several times in this article. For now, we also point out several features:

- The leading term,  $B_0(N) = (3N)^{1/3}$ , is always an overestimate, being 44% too high at  $N = 1$ , with the error decreasing with increasing  $N$ .
- Inclusion of the second term reduces the error to a 6% underestimate for  $N = 1$ , and now the sign of the error varies. This is almost always a better approximation than  $B_0(N)$ , except near  $N = 0$ , where  $B_0$  gives the exact answer, while  $B_1 = -1/2$ .
- The first two terms are smooth functions of  $N$ , but the exact partial sum  $S_N$  has kinks wherever  $S_N$  passes through an integer.

To understand how the series of Eq. (8) is generated and what the next (more complicated) terms are, we refer to the excellent book by Ergler[31].

## II. BACKGROUND AND NOTATION

### A. Kohn-Sham DFT

The formal basis of DFT was established first by Hohenberg and Kohn[32], but we use the more general formulation of Levy here[11, 12]. The ground-state energy of any electronic system can be found from an exact variational principle in the density:

$$E = \min_n \left\{ F[n] + \int d^3r n(\mathbf{r}) v(\mathbf{r}) \right\} \quad (9)$$

where  $v(\mathbf{r})$  is the one-body potential, the minimization is over all normalized non-negative densities with finite kinetic energy[12], and

$$F[n] = \min_{\Psi \rightarrow n} \langle \Psi | \hat{T} + \hat{V}_{ee} | \Psi \rangle, \quad (10)$$

where  $\hat{T}$  is the kinetic energy operator,  $\hat{V}_{ee}$  is the electron-electron repulsion, and the minimization is over all normalized antisymmetric wavefunctions.

The original DFT was that of Thomas-Fermi[33, 34], in which the kinetic energy of the electrons is approximated with a local approximation:

$$T^{\text{TF}}[n] = A_s \int d^3r n^{5/3}(\mathbf{r}) \quad (11)$$

where  $A_s = 3(3\pi^2)^{2/3}/10$ , and their interaction energy is approximated by the Hartree electrostatic self-energy of the density:

$$V_{ee}^{\text{TF}}[n] = U[n] = \frac{1}{2} \int d^3r \int d^3r' \frac{n(\mathbf{r}) n(\mathbf{r}')}{|\mathbf{r} - \mathbf{r}'|} \quad (12)$$

Applying such approximations to the total energy, and minimizing to find the density of a system, leads to self-consistent TF theory, which was used for several decades in materials calculations[35]. The TF equation for an atom is now iconic[33, 34, 36], and was solved numerically in the original papers. Energies are typically accurate to within about 10%, but the theory is too crude for modern chemical and materials purposes[35].

The variant in use in almost all modern electronic structure calculations is Kohn-Sham (KS) DFT, which posits a fictitious set of non-interacting electrons with the same ground-state density[1]. These electrons satisfy the Pauli principle and obey the KS equations:

$$\left\{ -\frac{1}{2} \nabla^2 + v_s(\mathbf{r}) \right\} \phi_i(\mathbf{r}) = \epsilon_i \phi_i(\mathbf{r}). \quad (13)$$

Writing the energy in terms of these orbitals,

$$E = T_s + U + V + E_{xc}, \quad (14)$$

where  $T_s$  is the kinetic energy of the KS orbitals,  $U$  their Hartree energy, and  $E_{xc}$  is defined by Eq. (14). For simplicity, we write all equations here in terms of DFT, but in practice, and in our calculations, we use spin-DFT[37].

Kohn and Sham also wrote down the most primitive approximation to use in their equations[1], the local density approximation (LDA) for XC:

$$E_{\text{xc}}^{\text{LDA}} = \int d^3r e_{\text{xc}}^{\text{unif}}(n(\mathbf{r})) \quad (15)$$

where  $e_{\text{xc}}^{\text{unif}}(n)$  is the XC energy density of a uniform gas of density  $n$ , which is now known very accurately[38–40]. This was used for a generation in solid-state physics[41, 42], but almost always significantly overbinds molecules, so it never became widespread in chemistry. However, most of the properties of molecules in LDA calculations (such as bond lengths and vibrational frequencies) are surprisingly accurate[41].

At first, it was thought that LDA might be improved using the gradient expansion[43], which includes the leading corrections to the LDA energy for a sufficiently slowly varying gas:

$$E_{\text{xc}}^{\text{GEA}} = E_{\text{xc}}^{\text{LDA}} + \int d^3r g_{\text{xc}}(n) s^2(\mathbf{r}) \quad (16)$$

where  $s = |\nabla n|/(2k_{\text{F}}n)$ ,  $k_{\text{F}}$  is the local Fermi wavevector, and  $g_{\text{xc}}(n)$  has been derived from many-body theory[44, 45], at least in the high-density limit. However, in many cases, these corrections worsened LDA results for atoms and molecules. This lead ultimately to the development of modern *generalized* gradient approximations[46], which include more general functions of  $s$  (but not higher gradients), and led to the widespread use of KS-DFT in chemistry and materials today[47]. In this language, we can then understand that  $T^{\text{TF}} = T_{\text{s}}^{\text{LDA}}$ , i.e., the Thomas-Fermi theory approximates the kinetic energy as a local functional of the density for non-interacting electrons.

The standard way to think about XC is in terms of the strength of the Coulomb interaction[3]. In DFT, we put a coupling constant  $\lambda$  in front of  $V_{\text{ee}}$  and imagine varying it, keeping the density fixed. Then, for finite systems,

$$E_{\text{xc}}^{\lambda} = \lambda E_{\text{x}} + E_{\text{c}}^{\lambda} \quad (17)$$

where the correlation energy contains only  $\lambda^2$  and higher powers of  $\lambda$ . Truncation at first order yields exact exchange, the DFT version of Hartree-Fock[48], which yields ground-state energies almost identical to those of HF[49].

One can relate this  $\lambda$ -dependence to coordinate scaling of the density[50]:

$$n_{\gamma}(\mathbf{r}) = \gamma^3 n(\gamma\mathbf{r}), \quad 0 < \gamma < \infty \quad (18)$$

via

$$E_{\text{xc}}^{\lambda}[n] = \lambda^2 E_{\text{xc}}[n_{1/\lambda}]. \quad (19)$$

This can be used to write  $E_{\text{xc}}$  entirely in terms of a purely potential contribution, the infamous adiabatic connection formula[51–53]. Furthermore, in the absence of degeneracies,

$$T_{\text{s}}[n] = \lim_{\gamma \rightarrow \infty} F[n_{\gamma}]/\gamma^2, \quad (20)$$

and

$$E_{\text{x}}[n] = \lim_{\gamma \rightarrow \infty} E_{\text{xc}}[n_{\gamma}]/\gamma. \quad (21)$$

## B. Z-scaling

We begin with a definition of scaling to large  $Z$ . For any system of  $N$  non-relativistic electrons with one-body potential  $v(\mathbf{r})$ , we define a  $\zeta$ -scaled system[13]:

$$v_{\zeta}(\mathbf{r}) = \zeta^{4/3} v(\zeta^{1/3}\mathbf{r}), \quad N_{\zeta} = \zeta N, \quad (22)$$

where  $\zeta$  is a positive real number. As  $\zeta \rightarrow \infty$ , this corresponds to simultaneously scaling the coordinates and increasing the particle number. For atoms or ions,

$$v(\mathbf{r}) = -Z/r, \quad v_{\zeta}(\mathbf{r}) = -\zeta Z/r, \quad (23)$$

i.e.,  $\zeta$ -scaling is simply the same as changing the number of protons and electrons by the same fraction. For molecules and solids, all nuclear separations  $\mathbf{R}$  also scale as  $\mathbf{R}/\zeta^{1/3}$ . The complementary density scaling is

$$n_{\zeta}(\mathbf{r}) = \zeta^2 n(\zeta^{1/3}\mathbf{r}). \quad (24)$$

This differs from the usual coordinate scaling of Eq. (18) as the particle number also changes. Analogous to that case, the  $\zeta$ -scaled density is, in general, *not* the ground-state density of the  $\zeta$ -scaled potential, except within the TF approximation.

## C. Lieb-Simon theorem

Lieb and Simon[54] rigorously proved that, as  $\zeta \rightarrow \infty$ ,

$$\lim_{\zeta \rightarrow \infty} \frac{E(\zeta) - E^{\text{TF}}(\zeta)}{E(\zeta)} \rightarrow 0 \quad (25)$$

for all non-relativistic Coulombic systems. For example, the percentage error of the energy in a TF calculation for an atom vanishes for large  $Z$ . Moreover, any well-behaved integral over the density of the form[12]

$$I = \int d^3r f(n(\mathbf{r}), \mathbf{r}) \quad (26)$$

will also become relatively exact. Although  $n^{\text{TF}}(\mathbf{r})$  has many well-known deficiencies (divergence at the nucleus, non-exponential decay at large distances, missing quantum oscillations) integrals such as  $I$  over  $n^{\text{TF}}(\mathbf{r})$  have vanishing relative error in this limit.

Without taking too large a leap, we assume the LS result is also true for non-interacting electrons in any potential[55], yielding

$$\frac{T_{\text{s}}(\zeta) - T_{\text{s}}^{\text{TF}}(\zeta)}{T_{\text{s}}(\zeta)} \rightarrow 0, \quad \zeta \rightarrow \infty \quad (27)$$

again, a universal limit of all systems. Thus any approximation that fails to satisfy this limit is unlikely to be a useful starting point for a large variety of systems.



#### D. Illustration: Hydrogenic atoms

The simplest useful example of  $T_s$  is to consider non-interacting electrons in a hydrogen potential,  $-1/r$ . Their energies are  $-1/2n^2$ , where  $n$  is the principal quantum number. Via the virial theorem,  $T_s = -E$ , and accounting for double occupation of the orbitals, in fact

$$T_s(N) = \frac{1}{2} S_{N/2} \quad (28)$$

where  $S_N$  is the partial sum from the introduction. Thus our purely mathematical example is in fact a relevant example. The TF density for this problem is simply:

$$n^{\text{TF}}(r) = \frac{4Z}{\pi^2 r_c^3} \left( \frac{r_c}{r} - 1 \right)^{3/2} \Theta(r_c - r), \quad (29)$$

where  $r_c = (18/Z)^{1/3}$ , and  $\Theta$  is the Heaviside step function. This situation is similar to the interacting case, in that the TF density is singular at the origin, missing oscillations, and does not decay correctly at large  $r$ . Insertion of Eq. (29) into Eq. (11) yields precisely  $(3N/2)^{1/3}/2$ , the leading term in the expansion for large  $N$ . This is consistent with Eq. (27). Thus, this reasoning says that, for an orbital-free theory to take advantage of the LS result, it should recover both this value and the next correction[56] ( $-1/2$ ) in the large- $Z$  limit. Of course, this is unlikely to be sufficient to determine a usefully accurate orbital-free DFT. But if the reasoning commonly applied to XC is applied to this problem, i.e., that approximate functionals should build in those conditions that they can satisfy, it is a *necessary* exact condition. No approximate kinetic energy functional known at present produces the correct value for these coefficients for all electronic systems[36].

#### E. Exchange-correlation analog

This section addresses a fundamental question about DFT in chemistry and materials science, which is: How can such simple approximations, such as LDA, GGA or even hybrids, possibly yield usefully accurate results for such a demanding many-body problem? While their failures for many specific properties and systems are myriad, their successes are legion. How can this be, since everyone knows how demanding and complicated the many-body problem is?

The seeds of the answer are in the Lieb-Simon theorem. As  $Z$  grows, local approximations become more accurate for the energy and other integrated quantities (but not pointwise for densities, energy-densities, or potentials). The many-body problem becomes simple in two extremes:  $N = 1$  and  $N \rightarrow \infty$ . All the detailed behavior of the wavefunctions is averaged away, as quantum oscillations become more and more rapid in space, having less and less effect on system averages.

This then provides a systematic approach to constructing DFT approximations, but one which is entirely different from the traditional approach in terms of many-body theory and expansions in  $\lambda$ , the electron-electron interaction. The Thomas-Fermi approximation becomes relatively exact for large  $N$ . Note that we do not claim that our systems of interest have large  $N$ , and indeed, a direct large- $N$  expansion of the energy is often not sufficiently accurate. Instead, we apply the large- $N$  DFT approximation self-consistently to the problem at hand. We are using the density functional that is exact at large  $N$ , which is much more accurate than simply taking the large- $N$  behavior of our specific system. In terms of our hydrogenic illustration, a GGA for  $T_s$  can be constructed that automatically recovers the first two terms in the expansion of the energy, but that is more accurate for small  $N$  than the asymptotic expansion alone[36].

We now conjecture that the following statement is true for KS-DFT:

$$\lim_{\zeta \rightarrow \infty} \frac{E_{\text{xc}}(\zeta) - E_{\text{xc}}^{\text{LDA}}(\zeta)}{E_{\text{xc}}(\zeta)} \rightarrow 0. \quad (30)$$

We call this a conjecture, because the Lieb-Simon theorem for TF theory has been proven rigorously in a mathematical physics sense[57], but no such general demonstration yet exists for  $E_{\text{xc}}$ . However, all evidence suggests that this conjecture is correct. For example, few would doubt that, in a limit in which the number of particles is growing,  $E_c/E_x \rightarrow 0$ , so that the statement need only be proven for  $E_x$ . This was demonstrated very carefully by Schwinger[17, 18, 58–64] for atoms, and detailed in the pioneering book of Englert[31]. It was later proven rigorously for atoms[20]. It can be proven for all systems if the singularity at the nuclei is smoothed[19], but no general mathematical proof has been given for Coulomb interactions. For our purposes, this is sufficient.

Virtually all modern XC approximations reduce to  $E_x^{\text{LDA}}$  for uniform densities, which means they also do so for inhomogeneous systems as  $\zeta \rightarrow \infty$ . Assuming the conjecture is correct, this makes sense as  $E_x^{\text{LDA}}$  is then a *universal* limit for all systems, and its relevance has nothing to do with the rapidity of the density variation (which is never slow for realistic finite systems). By studying the exchange energies of noble gas atoms of increasing  $Z$ , one can[21] deduce  $E_x^{\text{LDA}}[n]$ , i.e., it is a simple limit of *all* systems, one in which the many-body problem becomes very difficult (the number of particles is diverging), but in which the density functional for the integrated quantity simplifies enormously.

As  $\zeta \rightarrow \infty$ , the coupling between electrons becomes weak, just as it happens for  $\gamma \rightarrow \infty$ , in coordinate scaling. Thus this limit is weakly correlated. But the number of particles is also growing, and the number of pair-interactions is growing even faster. In this limit,

$$V_{\text{ee}}[n_\zeta] \rightarrow \zeta^{7/3} U[n] + \zeta^{5/3} E_x^{\text{LDA}}[n] + \dots \quad (31)$$

If we compare this with the usual coordinate scaling, and speak in terms of the coupling constant, as  $\zeta$  grows, the

effective coupling constant is shrinking. But due to the increased number of interactions, the net effect is as given above. The analog to Eq. (20) using the Lieb-Simon theorem is

$$T_s^{\text{TF}}[n] = \lim_{\zeta \rightarrow \infty} F[n_\zeta]/\zeta^{7/3} \quad (32)$$

while for XC, the analog to Eq. (21) is

$$E_x^{\text{LDA}}[n] = \lim_{\zeta \rightarrow \infty} E_{\text{xc}}[n_\zeta]/\zeta^{5/3}. \quad (33)$$

We can then argue that, if standard DFT approximations work reasonably well for weakly-correlated systems, it is because the density-dependence of the XC energy, found self-consistently in the KS scheme, is well-approximated by the limiting density functional. Most molecular systems at or near equilibrium bond lengths are weakly correlated, so LDA yields usefully accurate values in this region. While LDA is insufficiently accurate for the energy difference between an equilibrium bond and dissociated atoms, its error is extremely systematic, and the next correction to the energy in the form of a GGA works reasonably well.

This is entirely analogous to the starting approximation for most many-body treatments. Hartree-Fock becomes relatively exact as the electron-electron repulsion becomes weak. But in practice we apply it directly to our many-electron system with the full electron-electron repulsion, and find usefully accurate descriptions (although not bond-energetics) from the self-consistent solution of those equations. In this sense, LDA is as non-empirical as HF, and is substantially more accurate for bond energies.

### F. Locality principle

Here we claim that a *locality* principle is at work in DFT: Many of the successes and failures of DFT approximations to XC can be understood in terms of the expansion of the functional around the large- $Z$ , i.e., local limit. The success of LDA for real materials (not slowly varying gases) has nothing to do with the uniform gas per se. It is a universal limit of *all* quantum systems, and that limit is most easily calculated from the uniform gas. The real question is: For real molecules and materials, does LDA dominate, and if so, how large are the corrections? LDA works as well (or as badly) as it does for weakly correlated systems because, for those systems, the density-dependence of the XC energy functional is moderately accurately approximated by its limiting form (i.e., a local one). For such systems, and only such systems, inclusion of the next correction should improve its accuracy. Thus most molecules and many materials at equilibrium are weakly correlated. LDA works reasonably well, and standard GGA's usually improve energetics substantially. On the other hand, static correlation is a signal that this expansion is failing, and hybrid functionals[6, 65] are a crude attempt to account for this.

We therefore define the beyond-local XC energy functional as

$$E_{\text{xc}}^{\text{BL}}[n] = E_{\text{xc}}[n] - E_{\text{xc}}^{\text{LDA}}[n] \quad (34)$$

and an obvious question arises: If LDA becomes relatively exact for  $E_{\text{xc}}$  at large  $\zeta$ , what approximation for  $E_{\text{xc}}^{\text{BL}}[n]$  becomes relatively exact in this limit? This is the natural expansion of which LDA is the leading order, and one can hope that accurate inclusion of the next order will lead to accurate energetics for weakly correlated systems. Presumably, standard GGA's are crude examples of such corrections.

### G. A simple example: Exchange

The answers for exchange are simple, and well-established[21]. In this case, for atoms,

$$E_x \rightarrow -A_x Z^{5/3} + B_x Z + \dots \quad (35)$$

The dominant term is exact within LDA, given by

$$E_x^{\text{LDA}}[n] = -\frac{3}{4} \left(\frac{3}{\pi}\right)^{1/3} \int d^3r n^{4/3}(\mathbf{r}) \quad (36)$$

To evaluate this, we write the TF atomic density in dimensionless form[31]:

$$n^{\text{TF}}(r) = \frac{Z^2}{4\pi a^3} f(x) \quad (37)$$

where  $x = Z^{1/3}r/a$  and  $a = (3\pi/4)^{2/3}/2$ . Inserting this into Eq. (36) yields[36]

$$A_x = \left(\frac{9}{2\pi^4}\right)^{1/3} M, \quad M = \int_0^\infty dx x^2 f^{4/3}(x) \quad (38)$$

where  $M$  is known numerically to be about 0.615434679[36]. Thus  $A_x \approx 0.2208274$ . The precise value of  $B_x$  has not been derived, but estimates for  $B_x$  have been extracted numerically by careful extrapolation to the large  $Z$  limit of atoms.  $B_x^{\text{LDA}} \approx 0$ , but  $B_x \approx 0.224$ , i.e., there is a large beyond-local contribution. The two most commonly used[4, 8] generalized gradient approximations for  $E_x$  recover this BC contribution rather accurately, whereas the gradient expansion for the slowly-varying gas, when applied as an approximation to atoms, is smaller by about a factor of 2[22, 66].

### H. Non-empirical constants

At this point, we make a small aside about what we mean by the term non-empirical. For simplicity, return to our mathematical example. Suppose we argue (or notice from examples) that the leading term must grow as  $N^{1/3}$ ,

and we use some set of tabulated values of  $S_N$  to fit the coefficient in  $B_0(N)$ . If we used just the point  $N = 1$ , we would get this coefficient quite wrong (1 instead of  $3^{1/3} \approx 1.4422$ ). If we use the first 10 points, we get a more accurate answer. But if, instead, we use tabulated values of  $S_N$  to extrapolate the  $N \rightarrow \infty$  value, we get our best estimate of the non-empirical value. Thus, by using tabulated values and the correct form of the expansion, we can estimate a non-empirical coefficient, even though we might not have the ability or energy to derive its value analytically. The larger the values of  $N$  that we use, and the more terms in the form, the more accurate our estimate can be. For example, knowing  $S_N$  for  $N = 1$  to 100, and the form  $AN^{1/3} + B$ , we can estimate  $A = 1.4458$  and  $B = 0.525$ , by using only the last 50 values. We denote the result as non-empirical, even though it has not been derived analytically, and we do not get the exact analytic value, just a best estimate of it.

Simple fitting (such as a polynomial fit) to a range of finite data, including small  $N$  but without accounting for the asymptotic analytic form, will usually produce a numerically more accurate value within the range of the data, but will fail as  $N$  grows larger, and might be disastrous when attempting to find the next correction. Note also that it is vital to know the correct form, to guarantee relative exactness as  $N$  grows, and to allow investigation of higher-order terms.

### III. ATOMIC CORRELATION

#### A. Data

##### 1. Quantum chemical data

We are almost ready to begin our analysis of the locality of the correlation energy. All our data will come from non-relativistic atomic calculations. Our starting point is the relatively recent publication of total correlation energies of spherical atoms[28] up to  $Z = 86$  and non-spherical ones[67] up to  $Z = 36$ . These add to the well-known benchmark set[68] up to  $Z = 18$ , although they are not quite as accurate. It is the existence of these results that make the following analysis possible. Their values appear (with many others) in Table I, and are plotted in Fig. 3, in the form of correlation energy per electron.

The behavior of correlation energies across rows, and how it changes as one goes down a column, will play an important role in our analysis, but the data set becomes sparse for large  $Z$ . We have therefore performed pure random-phase-approximation (RPA) calculations for all elements up to  $Z = 86$ , and these results are included in Fig. 3. We use this to ‘fill in’ gaps in the reference data set.

#### 2. RPA calculations

The adiabatic connection formula[51–53] combined with the fluctuation-dissipation theorem and RPA is fast becoming a *de facto* standard[69–71] for calculations of *nearly* quantum chemical accuracy energy differences. Unfortunately, it is well known that RPA gives poor estimates of *absolute* correlation energies. As we will show later, this erroneous contribution can, at least in the atomic systems considered here, be cancelled by a simple fit, Eq. ((67)), depending on the number of electrons only. This thus renders corrected RPA suitable for accurate correlation energy calculations of atoms, on a par with the most accurate quantum chemical benchmarks.

RPA energies are calculated using the ACFD correlation energy formula

$$E_C = \int_0^1 d\lambda \int d^3r d^3r' \frac{n_{2c}^\lambda(\mathbf{r}, \mathbf{r}')}{2|\mathbf{r} - \mathbf{r}'|} \quad (39)$$

Here the pair-density  $n_{2c}^\lambda$  is found from the fluctuation dissipation theorem via

$$n_{2c}^\lambda(\mathbf{r}, \mathbf{r}') = \int_0^\infty \frac{d\omega}{\pi} [\chi^\lambda(\mathbf{r}, \mathbf{r}'; i\omega) - \chi^0(\mathbf{r}, \mathbf{r}'; i\omega)] \quad (40)$$

$$\chi^0 = 2\Re \sum_i f_i \phi_i(\mathbf{r}) \phi_i(\mathbf{r}') G(\mathbf{r}, \mathbf{r}'; \epsilon_i - i\omega) \quad (41)$$

$$\chi^\lambda = \chi^0 + \lambda \chi^0 \star \frac{1}{|\mathbf{r} - \mathbf{r}'|} \star \chi^\lambda \quad (42)$$

where stars indicate spatial convolutions. The non-interacting response  $\chi_0$  takes as input the Kohn-Sham orbitals  $\phi_i$  and energies  $\epsilon_i$  obeying  $\{-\frac{1}{2}\nabla^2 + v_s - \epsilon_i\}\phi_i = 0$ ; and KS Greens functions  $G(\mathbf{r}, \mathbf{r}'; \epsilon_i - \omega)$  obeying  $\{-\frac{1}{2}\nabla^2 + v_s - \epsilon_i + i\omega\}G(\mathbf{r}, \mathbf{r}'; \epsilon_i - i\omega) = -\delta(\mathbf{r} - \mathbf{r}')$ . We work from spherical and spin symmetric groundstates which make all calculations essentially one-dimensional. All equations can thus be carried out using a large radial grid which helps to reduce numerical errors in (39). Errors are estimated to be well under 1.1 mHa per electron. We use the same algorithms and code as previous work[72, 73]

Equation (39) is an indirect orbital function which formally maps a Kohn-Sham potential  $v_s$  and orbital occupation factors  $f_i$  to a correlation energy. We must thus start from a reasonably accurate potential if we are to expect accurate energies. For this work, we perform RPA calculations using strictly spherical Kohn-Sham potentials calculated using LEXX[72] theory, extended to  $d$  and  $f$  shells. For most elements, the occupation factors are assigned according to Hund’s rules, in accordance with theoretical and experimental evidence. For the transition metals we use the lowest energy orbital filling (in exact exchange theory) of the  $s$  and  $d$  shells (e.g.  $4s^1 3d^{10}$  for Cu and  $5s^1 4d^4$  for Nb), which allow ready comparison with the results of McCarthy and Thakkar[67]. For the atoms in Row 6 we simply fill the orbitals in according to Hund’s rules to avoid issues of (near-)degeneracy.

Ideally the orbitals would be calculated on the exact Kohn-Sham potential  $v_s(\mathbf{r})$ , but this is available for only a very limited number of atoms, forcing us to use an appropriate approximation to the potential. The LEXX potential was chosen due to its good asymptotic form and inclusion of static correlation in open shell systems. To ensure our RPA energies are appropriate we performed some additional tests to study dependence on the potential. Firstly, for C and F we evaluated RPA energies using both the exact[74] potential and the LEXX potential and found the difference to be less than 0.3 mHa per electron. We also compared energies calculated using the PBE potential and LEXX potential across many species and found a maximum difference of 1.0 mHa per electron, a likely worst case scenario. We thus assume our total error (numerical and error from the potential) to be under 1.5 mHa per electron or 3%, whichever is the larger. This gives us, through RPA and the corrections discussed later, accurate benchmarks for all non-relativistic atoms with up to 86 electrons.

### 3. DFT calculations

At the opposite end of the scale, one can perform atomic DFT calculations of correlation energies rather simply, and go to much larger  $Z$  than with correlated wavefunction treatments. For the purposes of our study, we include all  $Z$  up to 86, and use both LDA and PBE results. We use the PW92 parametrization of the uniform gas[40], the relevance of which will be discussed below. We include PBE because, as shown below, its form mimics that of the exact functional in the large  $Z$  limit, so that the large- $Z$  behavior can be most easily extracted by comparison with that approximation.

### 4. Results

Tables I and II list all our results. In Fig 3, we plot correlation energies per electron as a function of  $Z$ , as well as the RPA and LDA results. The shapes are well-known and unsurprising. The RPA significantly overcorrelates the atoms, and the LDA is even worse. Many quantum chemists question the value of LDA for such calculations, as the relevance of the uniform gas for such systems is far from obvious. For now, we simply note that it is unclear if the correlation energy per electron is approaching a constant for sufficiently large  $Z$ . In fact, we argue below that this is definitely *not* the case.

Note that the difference between HF energies [67, 75] and Kohn-Sham exact exchange energies (as computed in our work) is smaller than other errors, so we ignore this difference here.

TABLE I. Negative of atomic correlation energies per electron in Ha. Final digit is approximate and all numerical errors are estimated to be under 1 mHa per electron. “Bench” is benchmark data from Refs. 28, 67, and 68 and “acRPA” is asymptotically corrected RPA. Errors on “Bench” are estimated to be within 2.2% for  $Z \leq 54$  and 3.5% for larger atoms[28, 67] while errors on “acRPA” could be up to 5.5% (including numerical errors and differences between EXX and HF energies).

$N$	Bench	RPA	Err	acRPA	Err	LDA	PBE	Err
1	0.0	20.9	20.9	-5.0	-5.0	21.7	5.7	5.7
2	21.0	42.0	21.0	18.6	-2.4	55.5	20.5	-0.5
3	15.1	37.8	22.7	15.4	0.3	50.1	17.0	1.9
4	23.6	45.6	22.0	23.6	0.0	55.9	21.4	-2.2
5	25.0	45.5	20.5	23.8	-1.2	57.9	23.1	-1.9
6	26.1	46.6	20.6	25.1	-0.9	59.5	24.5	-1.6
7	26.9	48.7	21.8	27.4	0.5	60.8	25.5	-1.4
8	32.2	51.9	19.7	30.7	-1.6	66.7	29.5	-2.7
9	36.1	55.8	19.7	34.6	-1.5	70.9	32.5	-3.6
10	39.1	60.1	21.0	39.0	-0.1	74.0	34.7	-4.4
11	36.0	57.2	21.1	36.2	0.1	72.7	33.5	-2.5
12	36.6	57.5	20.9	36.5	-0.1	73.9	34.1	-2.5
13	36.2	56.6	20.4	35.7	-0.5	74.0	34.3	-1.9
14	36.1	56.5	20.4	35.7	-0.5	74.0	34.6	-1.5
15	36.1	57.1	21.1	36.3	0.2	74.2	35.0	-1.1
16	37.9	58.2	20.3	37.4	-0.5	76.3	36.6	-1.3
17	39.3	59.7	20.4	38.9	-0.4	77.8	38.0	-1.3
18	40.3	61.5	21.2	40.8	0.4	79.1	39.1	-1.2
19	40.2	61.1	20.9	40.4	0.2	78.4	38.5	-1.7
20	41.3	62.1	20.8	41.4	0.1	78.8	38.7	-2.6
21	42.2	62.7	20.5	42.0	-0.2	79.6	39.3	-2.8
22	42.9	63.4	20.5	42.7	-0.2	80.3	40.0	-2.9
23	43.7	64.3	20.6	43.7	-0.0	80.1	–	–
24	44.6	65.4	20.9	44.8	0.2	80.7	41.0	-3.6
25	45.2	66.7	21.5	46.0	0.8	82.1	41.7	-3.5
26	47.5	68.2	20.7	47.6	0.1	83.7	42.9	-4.6
27	49.1	69.8	20.6	49.2	0.0	85.5	44.5	-4.7
28	50.9	71.5	20.6	50.9	0.0	86.7	45.4	-5.5
29	54.6	73.3	18.7	52.7	-1.9	87.7	46.2	-8.4
30	54.0	75.2	21.2	54.7	0.7	88.4	46.7	-7.3
31	52.7	73.5	20.7	52.9	0.2	88.6	46.8	-5.9
32	51.8	72.4	20.6	51.9	0.1	88.6	47.0	-4.7
33	51.0	71.8	20.8	51.3	0.2	88.7	47.2	-3.8
34	51.2	71.5	20.4	51.0	-0.2	89.6	47.9	-3.3
35	51.3	71.6	20.3	51.1	-0.2	90.3	48.5	-2.8
36	51.4	71.9	20.5	51.4	0.0	90.8	49.0	-2.4

## B. Theory

We now test the locality conjecture for correlation, and use it to extract trends in Fig 3 and Table I. The conjecture implies that

$$E_c[n_\zeta] \rightarrow E_c^{\text{LDA}}[n_\zeta^{\text{TF}}], \quad \zeta \rightarrow \infty. \quad (43)$$

Thus we begin with the local density approximation, which uses the correlation energy of a uniform gas:

$$E_c^{\text{LDA}}[n] = \int d^3r n(\mathbf{r}) \epsilon_c^{\text{unif}}(n(\mathbf{r})), \quad (44)$$



TABLE II. Same as Table I, but larger  $Z$ .

$N$	Bench	RPA	Err	acRPA	Err	LDA	PBE	Err
37	—	71.2	20.5	50.7	—	90.4	48.6	-2.1
38	51.0	71.4	20.3	50.9	-0.2	90.6	48.7	-2.4
39	—	71.5	20.5	51.0	—	90.8	48.9	-2.2
40	—	71.6	20.5	51.1	—	91.0	49.1	-2.0
41	—	71.8	20.5	51.3	—	90.7	49.3	-2.0
42	—	72.1	20.5	51.6	—	90.8	—	—
43	—	72.5	20.5	52.1	—	91.6	49.9	-2.2
44	—	73.0	20.4	52.6	—	92.6	50.9	-1.6
45	—	73.6	20.4	53.2	—	93.3	51.5	-1.6
46	55.3	74.3	19.0	53.8	-1.4	94.4	52.5	-2.8
47	—	75.0	20.4	54.5	—	94.5	52.6	-1.9
48	55.2	75.7	20.5	55.3	0.1	94.8	52.8	-2.4
49	—	75.2	20.4	54.8	—	94.8	52.8	-2.0
50	—	75.0	20.4	54.6	—	94.8	52.9	-1.6
51	—	75.0	20.4	54.5	—	94.8	53.0	-1.6
52	—	75.1	20.4	54.7	—	95.3	53.4	-1.3
53	—	75.4	20.4	55.0	—	95.6	53.7	-1.3
54	55.6	75.9	20.3	55.5	-0.1	95.9	54.0	-1.5
55	—	76.2	20.4	55.8	—	95.6	53.7	-2.1
56	55.8	76.5	20.7	56.1	0.3	95.7	53.7	-2.1
57	—	77.1	20.4	56.7	—	95.8	53.9	-2.8
58	—	77.9	20.4	57.5	—	96.4	54.4	-3.1
59	—	78.7	20.4	58.3	—	96.7	54.7	-3.5
60	—	79.4	20.4	59.0	—	97.1	55.0	-4.0
61	—	80.1	20.4	59.7	—	97.4	55.3	-4.4
62	—	80.9	20.4	60.5	—	97.7	55.6	-4.9
63	—	81.7	20.4	61.3	—	98.0	55.9	-5.4
64	—	82.5	20.4	62.1	—	98.1	56.0	-6.1
65	—	83.4	20.4	63.0	—	99.2	56.9	-6.2
66	—	84.3	20.4	64.0	—	99.7	57.3	-6.6
67	—	85.3	20.4	64.9	—	100.2	57.8	-7.2
68	—	86.3	20.4	65.9	—	—	—	—
69	—	87.3	20.3	67.0	—	101.1	58.6	-8.4
70	67.0	88.4	21.4	68.1	1.0	101.6	59.0	-8.1
71	—	87.3	20.3	67.0	—	101.7	59.1	-7.9
72	—	86.4	20.3	66.1	—	101.9	59.2	-6.8
73	—	85.7	20.3	65.3	—	102.0	59.4	-5.9
74	—	85.2	20.3	64.9	—	102.1	59.5	-5.3
75	—	84.9	20.3	64.5	—	102.2	59.7	-4.9
76	—	84.7	20.3	64.4	—	102.7	60.0	-4.3
77	—	84.6	20.3	64.3	—	103.1	60.4	-3.9
78	—	84.6	20.3	64.3	—	103.6	60.9	-3.4
79	—	84.7	20.3	64.4	—	103.9	61.2	-3.2
80	64.7	84.8	20.1	64.5	-0.2	104.0	61.3	-3.4
81	—	84.3	20.3	64.0	—	104.0	61.3	-2.7
82	—	84.0	20.3	63.6	—	104.0	61.3	-2.3
83	—	83.8	20.3	63.4	—	103.9	61.3	-2.1
84	—	83.7	20.3	63.4	—	104.2	61.5	-1.8
85	—	83.7	20.3	63.4	—	104.4	61.7	-1.7
86	64.2	83.9	19.6	63.6	-0.7	104.6	61.9	-2.3

where  $\epsilon_c^{\text{unif}}(n)$  is the correlation energy per electron. This is a non-trivial function of the density that is now well-known from many-body theory and quantum Monte Carlo simulations of the uniform gas[38]. There are several almost identical parametrizations[39, 40] in common use. Our interest is the large- $\zeta$  limit, which is dominated by high densities. In a landmark of electronic structure

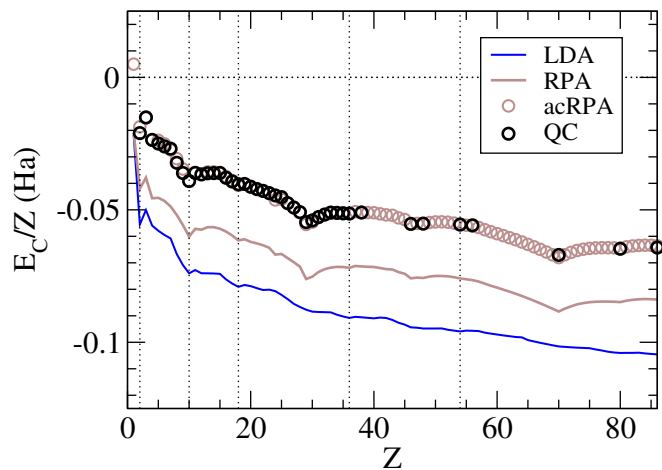


FIG. 3. Correlation energy per electron versus  $Z$  for accurate quantum chemistry (QC) calculations (black circles), the RPA (brown solid line), corrected RPA data (brown circles), and the local density approximation (LDA) of DFT. Circle size matches the maximum reported error of QC data.

theory, Gell-Mann and Brueckner[76] applied the random phase approximation (RPA) to the uniform gas to find:

$$\epsilon_c^{\text{unif}} = c_0 \ln r_s - c_1 + \dots, \quad r_s \rightarrow 0 \quad (45)$$

where  $r_s = (3/(4\pi n))^{1/3}$  is the Wigner-Seitz radius of density  $n$ ,  $c_0 = 0.031091$ , and  $c_1^{\text{RPA}} = 0.07082$ . In fact, Eq. (45) yields the exact high-density limit if  $c_1 = 0.04664$ , the correction from RPA being due to second-order exchange[77]. But, as is clear in Fig. 3, LDA[1] greatly overestimates the magnitude of the correlation energy of atoms (factor of 2 or more). For atoms with large  $Z$ , insert  $n^{\text{TF}}(\mathbf{r})$  into Eq. (44) to find:

$$E_c^{\text{LDA}} = -A_c Z \ln Z + B_c^{\text{LDA}} Z + \dots, \quad (46)$$

where  $A_c = 2c_0/3 = 0.02073$ .  $B_c^{\text{LDA}}$  is found by considering the contributions linear in  $Z$  generated by replacing Eq. (37) in the high-density limit of  $E_c^{\text{LDA}}[n]$ . As a result,

$$B_c^{\text{LDA}} = \frac{c_0}{3} [\ln(3a^3) - I_2] - c_1, \quad (47)$$

where

$$I_2 = \int_0^\infty dx f(x) \ln(f(x)), \quad (48)$$

and is known numerically to be about -3.331462[36]. This yields

$$B_c^{\text{LDA}} = -0.00451, \quad (49)$$

as reported in Ref. [66].

The locality conjecture, applied to correlation alone, implies that the leading term of Eq. (46) is exact. In fact, this has been proven for atoms relatively recently[29],

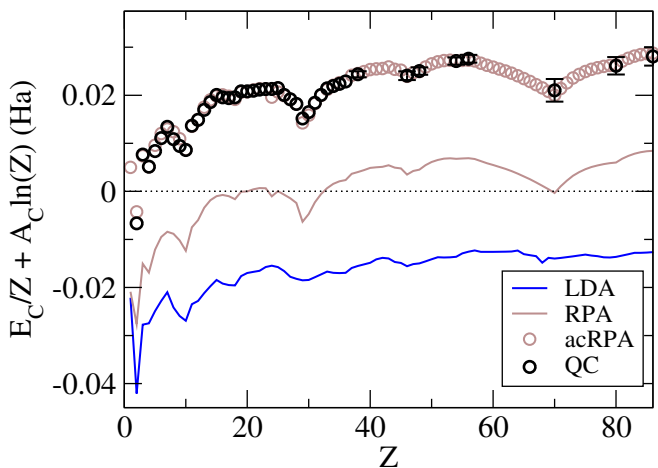


FIG. 4. Asymptotically corrected correlation energy per electron versus  $Z$  for accurate quantum chemistry (QC) calculations (black circles), the RPA (brown solid line), corrected RPA data (brown circles), and LDA.

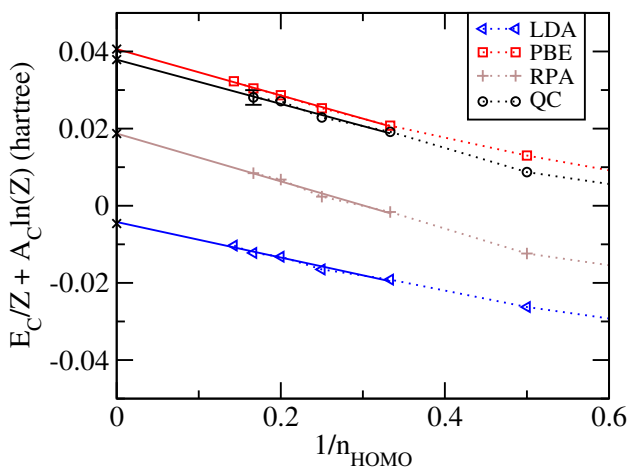


FIG. 5. Asymptotically-corrected correlation energy per electron as a function of inverse highest occupied shell for noble gases, for accurate quantum chemistry data (QC) and within RPA, LDA and PBE. For QC, the error for Rn is shown, others are smaller than data point size.

which shows definitively that the curves in Fig. 3 do not saturate. It also suggests we define:

$$e_{AC}(Z) = (E_C + A_C \ln Z)/Z \quad (50)$$

as the asymptotically-corrected correlation energy per electron. This is plotted in Fig. 4. Now the curves do appear to saturate, although the oscillations across open shells make accurate extrapolation of the large- $Z$  limit very difficult. For any such curve, we define

$$B_C = \lim_{Z \rightarrow \infty} e_{AC}(Z), \quad (51)$$

and try to estimate this value as accurately as possible. This will be the subject of the next section.

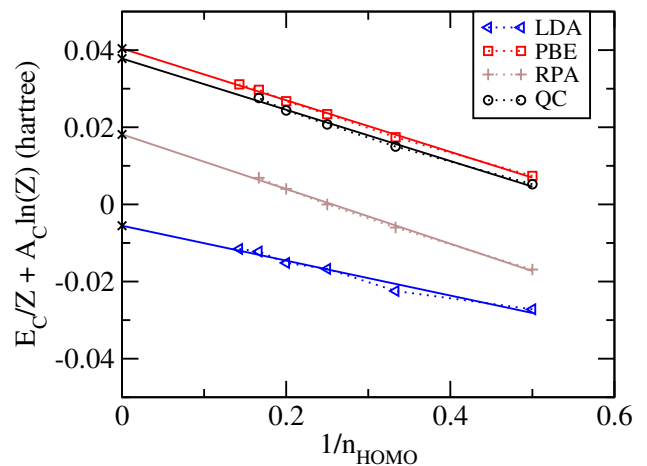


FIG. 6. Same as Fig. 5, but for alkali earths.

But to get a quick idea, using techniques that have worked for exchange[21, 36], we largely eliminate the effect of shell structure by taking only noble gas atoms, and plot as a function of  $1/n_{\text{HOMO}}$ , the principal quantum number of the highest occupied shell, as in Fig. 5. Clearly, the RPA and LDA values of  $B_C$  are quite different from the exact value. (The PBE correlation functional[8] is included, as its asymptotic behavior is almost perfectly parallel to the benchmark data, and we use this in the next section to improve our extrapolation.) Repeating the procedure for alkali earths shows that almost identical results occur, as shown in Fig. 6.

To make the extrapolation more accurate, first notice that the data oscillate slightly around each fit, with every other point being above or below. This reflects the double-step in the periodic table between the appearance of new rows, and ignoring this effect reduces the accuracy of an extrapolation. To account for this, while still analyzing atoms down a given column, we define

$$\tilde{n}^{nob}(Z) = (6Z + 8)^{1/3} - 2, \quad (52)$$

which smoothly interpolates  $n_{\text{HOMO}}$  between even and odd noble gas atoms, and is asymptotically correct as  $Z \rightarrow \infty$ . Writing

$$e_{AC}^{nob} = B_C^{nob} - C_C^{nob}/\tilde{n}^{nob}(Z), \quad (53)$$

we find  $B_C^{nob} = 0.0371$  and  $C_C^{nob} = -0.0536$ . Repeating the fit for the alkali earths (where we use  $\tilde{n}^{nob}(Z-2) + 1$  instead of  $\tilde{n}^{nob}(Z)$  in Eq. (53)), we find  $B_C^{AE} = 0.0378$  and  $C_C^{AE} = -0.0644$ , reflecting a consistency in the value of  $B_C$  extracted from either series. In the next section, we construct an even more reliable extrapolation method.

Having identified that  $B_C$  appears to approach a finite value, in the section we make a variety of constructions in order to estimate its value as accurately and reliably as possible from the available data. We also use some of the same techniques to fill in large- $Z$  non-spherical atomic correlation energies.

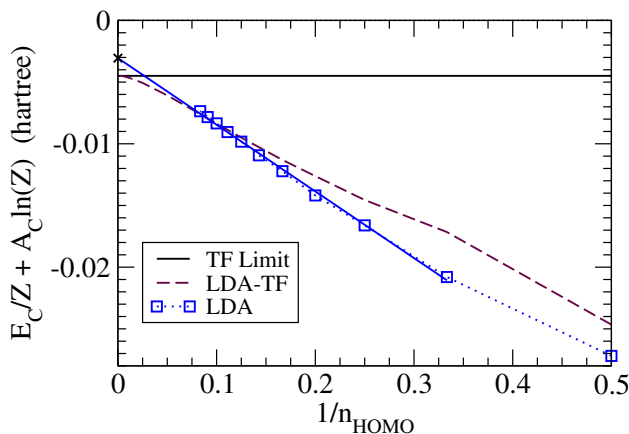


FIG. 7. Asymptotically corrected-correlation energy per electron versus  $1/n_{\text{HOMO}}$ , for alkali earth Be ( $n_{\text{HOMO}} = 2$ ) and averaged over noble gases and alkali earths for  $n_{\text{HOMO}} \geq 3$ . Shown are self-consistent LDA energies for up to  $n_{\text{HOMO}} = 12$  (blue squares) and LDA evaluated with Thomas-Fermi density (dashed line). The horizontal line is at the analytic value of  $B_C^{\text{LDA}}$ .

### C. Testing extrapolation methods on LDA

As an obvious test of our numerical extrapolation methods, we consider self-consistent LDA calculations for neutral atoms. Because such calculations are of irrelevant computational cost, we enlarge the data set up to  $Z = 460$ . This is the 12th row of the non-relativistic periodic table, assuming Madelung's rule continues indefinitely. Note that any calculations beyond  $Z = 100$  are simply a mathematical device to reduce the range of  $Z$  over which we extrapolate.

Because we can go to much larger  $Z$ , even/odd oscillations are less problematic and they can be largely eliminated by simply averaging over the noble gas and alkali earth atoms in a given row. These are both spherical (and so appear in our original QC data set) and not spin polarized. In Fig. 7, we plot the results of self-consistent LDA calculations (points connected by dashed line) and the LDA energy evaluated on the TF density for each value of  $Z$ , as well as marking the analytical limit from Eq. (47). One can see that even the solid line exhibits some structure for  $1/n_{\text{HOMO}} < 0.1$ , due to the logarithmic terms in the high-density expansion of  $\epsilon_C^{\text{unif}}$ . The difference between the self-consistent and TF curves also appears to be non-linear in this region. To understand this, we expand the uniform gas energy in the high-density limit to the next two orders beyond Eq. (45):

$$\epsilon_C^{\text{LDA}} \rightarrow c_0 \log r_s - c_1 + c_2 r_s \log r_s + c_3 r_s, \quad (54)$$

where  $c_2 = 0.0066$  and  $c_3 = -0.0104$  are known from perturbation theory[40]. Inserting the TF density yields

$$e_{\text{AC}}^{\text{LDA}}[n^{\text{TF}}](Z) \rightarrow B_C^{\text{LDA}} + (\tilde{C}_C \ln Z + \tilde{D}_C)/Z^{2/3} \quad (55)$$

where

$$\tilde{C}_C = -\frac{2}{3}c_2 \langle r_s \rangle = -0.051, \quad (56)$$

and

$$\tilde{D}_C = [c_3 \langle r_s \rangle + c_2 \langle r_s \log(r_s) \rangle] = 0.207. \quad (57)$$

In these equations,  $r_s = a(3/f(x))^{1/3}$  is the local Wigner-Seitz radius of the TF density for  $Z = 1$ , and

$$\langle g \rangle = \int_{-\infty}^{\infty} dx x^2 f(x) g(x). \quad (58)$$

The important feature is that this expansion is ill-behaved. These next two terms have much larger coefficients than the leading terms of Eq. (45), and the following two terms probably diverge on the TF density. This poor behavior is inherited from the uniform gas and shows how unsuitable all but the leading terms of the LDA are for approximating the correlation energy of atoms. Furthermore, it causes the structure we see in the figure as  $Z \rightarrow \infty$ . Thus, the LDA is especially difficult to extrapolate accurately. Nonetheless, performing a naive application of the linear extrapolation for  $n_{\text{HOMO}} \geq 3$  yields -3.0 mHa, an underestimate of 1.5 mHa from the analytic value. Thus we expect no larger error from our extrapolation process.

### D. Accurate estimate of $B_C$

Finally, we perform the extrapolation that produces our best estimate for  $B_C$ . To achieve the maximum accuracy, we compare the accurate QC data with PBE results[8]. The primary reason is that the PBE functional was constructed to yield an accurate finite result in this limit, by correcting the LDA energy. Our use here is simply that we can extrapolate the difference between QC and PBE, while extracting the PBE result analytically. The parallel trends in  $n_{\text{HOMO}}$  for the PBE and QC in Figs. 5 and 6 imply that their difference tends to a constant. Thus the resulting fit ought to be almost exclusively a measure of  $B_C$ , with minimum influence from the details of the fit.

The PBE beyond-local correlation energy for spin-unpolarized densities is[8]

$$E_C^{\text{BL,PBE}}[n] = \int d^3r n(\mathbf{r}) h_C^{\text{PBE}}(r_s(\mathbf{r}), t(\mathbf{r})), \quad (59)$$

where  $t = |\nabla n|/(2k_s n)$  is the dimensionless gradient for correlation,  $\beta = 0.066725$ ,  $k_s = 2(3n/\pi)^{1/6}$  is the TF screening length, and

$$h_C^{\text{PBE}}(r_s, t) = c_0 \ln \left( 1 + \frac{\beta}{c_0} t^2 f_C(\tilde{A}t^2) \right), \quad (60)$$

where

$$f_C(y) = (1+y)/(1+y+y^2), \quad (61)$$

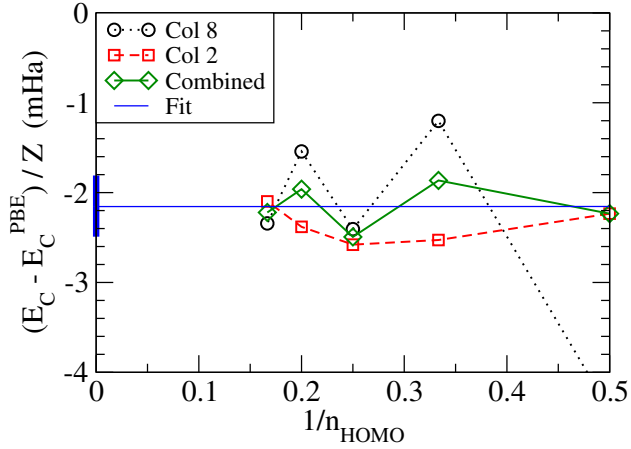


FIG. 8. Difference between the correlation energy-per-electron of QC data and the PBE. Differences for Column 2 and Column 8 plotted versus  $1/n_{\text{HOMO}}$ , along with the combined averages for  $n_{\text{HOMO}} = 3$  through  $n_{\text{HOMO}} = 6$ . Linear fit in blue, with error bar in the  $1/n_{\text{HOMO}} = 0$  asymptote shown as solid thick bar. Units in mHa.

and

$$\beta\tilde{A}^{-1} = c_0 [\exp(-\epsilon_C^{\text{unif}}/c_0) - 1], \quad (62)$$

This peculiar combination of functions results from requiring it to reduce to LDA for uniform densities, yield a finite value in the high-density limit of finite systems, and, when combined with PBE exchange, recover the LDA linear response for a uniform electron gas[8]. It is the first two conditions which ensure that it yields a finite value for  $B_C$  that differs from LDA.

$B_C^{\text{PBE}}$  is found by considering the contributions linear in  $Z$  generated by replacing Eq. (37) in the high-density large- $Z$  limit, where  $\tilde{A} \rightarrow 1/r_s$ ,  $y \rightarrow 0$ , and  $f_C \rightarrow 1$ . As a result,

$$\Delta B_C^{\text{PBE}} = c_0 I_3(\beta/c_0), \quad (63)$$

where

$$I_3(u) = \int_0^\infty dx x^2 f(x) \ln \left( 1 + \frac{u}{\sqrt{6}} \frac{df/dx}{f^{7/6}(x)} \right), \quad (64)$$

is a well-defined integral over the TF density[36]. For  $u = \beta/c_0 = 2.146119$ , we find  $I_3 = 1.411164$ , yielding

$$B_C^{\text{PBE}} = 0.03936. \quad (65)$$

in agreement with Ref. [66].

In Fig. 8, we plot the energy difference in mHa between QC and PBE per electron. Because the difference is so small, on this scale, the differences between noble gases and alkali earths are very visible, especially for odd rows. But their mean is seen to converge nicely. A fit yields

$$(E_C - E_C^{\text{PBE}})/Z = -0.00215(33) + 0.0000(11)/n_{\text{HOMO}}. \quad (66)$$

	AE	noble	analytic
LDA	-5.9(16)	-5.0(1.1)	-4.51
PBE	40.2(7)	40.2(5)	39.3
RPA	18.1(7)	18.7(1.4)	15.2
QC	37.8(9)	37.1(1.6)	N/A

TABLE III. Values for  $B_C$  in different approximations via numerical extrapolation and analytically. Reported errors, in parentheses, are statistical errors in the linear regression used to make the extrapolation. Errors in extrapolation can also be judged from the DFT cases where analytic results are known. The QC values are consistent with the best estimate of 37.1 mHa.

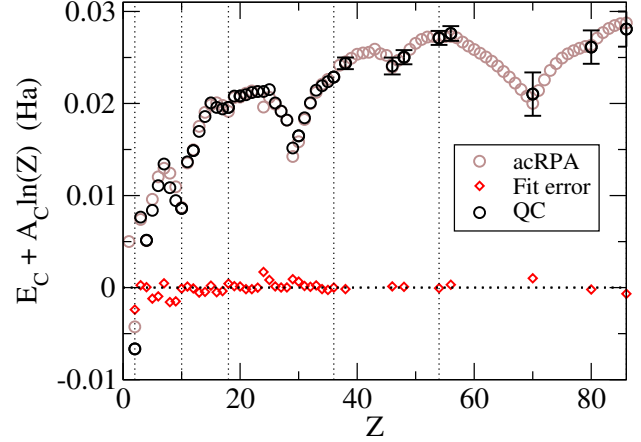


FIG. 9. Asymptotic correction of RPA data: black points are QC data, brown are RPA data corrected via Eq. (67), and red, their difference.

Combining the analytic result of Eq. (65) with this one, we conclude that the asymptotic value of  $B_C$  is 37.1 mHa. Table III compares the different estimates, showing their consistency, and suggesting the extrapolation error is no more than 1.5mHa.

## E. Corrections to RPA

There is considerable current interest in using RPA and beyond-RPA methods for quantum chemistry[78]. While many good features are known, a major drawback to pure RPA calculations for thermochemistry is the inaccuracy of RPA atomic energies, and its impact on atomization energies.

Unfortunately, the quantum chemical data becomes sparse for large  $Z$ , being limited to spherical atoms. However, our RPA calculations are less limited, and their error relative to the quantum chemical data set is relatively simple. We fit the error in RPA correlation energies extremely accurately with:

$$\Delta E_C^{\text{RPA}}/Z = 0.0199 + 0.00246/\tilde{n}^{\text{nob}}(Z), \quad (67)$$

where  $\tilde{n}^{\text{nob}}(Z)$  is given by Eq. (52). We denote by acRPA the RPA energies with the correction of Eq. (67) added



to them.

In Fig. 9, we plot both the accurate correlation energies and the acRPA values, and the residual error. Clearly, the fit is extremely accurate and errors become negligible for large enough  $Z$ . Finally, we note that the constant contribution to the fit, 19.9 mHa, is close (but different from) the error RPA makes for the correlation energy per electron in the high density limit of the uniform gas, 24.2 mHa, as discussed in Section III B. We can understand one contribution to this difference by considering the PBE for RPA correlation energies developed by Kurth and Perdew [79]. The expression of the corresponding enhancement factors is reported in Eq. (27) of Ref. [80], from which we readily obtain

$$B_C^{\text{PBE-RPA}} = 0.01518, \quad (68)$$

the difference with PBE being again due to RPA correlation energy of the uniform gas. Since the PBE construction uses the value of the gradient expansion coefficient  $\beta$  from the high-density limit in the RPA approximation, the *gradient* contributions to  $B_C^{\text{PBE}}$  and  $B_C^{\text{RPA}}$  are the same. Assuming this procedure is highly accurate for approximating RPA, the remaining difference is only 3 mHa - well within the numerical error bars for RPA correlation energies, estimated to be up to 4.6 mHa (3% of 84 mHa) for  $Z = 86$ .<sup>2</sup>

Note that this correction formula concerns the relation between an approximation to the many-electron problem and the exact result, and is entirely independent of any density functional analysis. Its value is that we can create an enhanced data-set of the QC data, plus RPA-corrected estimates for the larger open-shell atoms. We use acRPA for benchmark values wherever QC values are unavailable, i.e., the non-spherical atoms of Table II. Our simple atomic correction, Eq. (67), is remarkably accurate, as shown in Tables I and II, with few errors greater than 1 mHa. A scheme which reproduces this correction, but also works well for molecules at equilibrium bond lengths, would overcome the limitations of pure RPA. We suggest testing existing schemes for their behavior in the large- $Z$  limit, characterizing them by the value of  $B_C$ .

### F. Deviations from smooth functions of $Z$

In this final section, we study the deviations from smooth functions for both exchange and correlation throughout the periodic table. To create such smooth functions, we fit the alkali earth values with continuous functions of  $Z$ , and apply these functions for every value of  $Z$ .

<sup>2</sup> Additional numerical tests suggest that our RPA energies may be systematically over-estimated, which would reduce the discrepancy between theory and our calculations. However, as these possible systematic errors lie within the overall numerical error bars we do not attempt to correct for them.

As we know LDA becomes relatively exact for exchange for large  $Z$ , we define

$$e_{\text{AX}} = E_{\text{X}}/Z - A_{\text{X}} Z^{2/3}, \quad (69)$$

and fit OPM exchange energies for alkali earths with

$$e_{\text{AX}}^{\text{smooth}} = -(0.1466x^3 + 0.0314x^2 + 0.0823) \quad (70)$$

where  $x = 1 - Z^{-1/3}$ . This gives  $B_{\text{X}} = -0.260$  in agreement with a previous estimate of -0.24[21]. The value of -0.08 at  $Z = 1$  is somewhat off the actual value of -0.11, but gives a close fit to  $e_{\text{AX}}$  for all  $Z > 2$ . For correlation, we use the smoothed  $e_{\text{AC}}^{\text{AE}}(Z)$  of Eq. (53). Both the exchange and correlation forms are chosen to yield good fits even when  $Z$  is small.

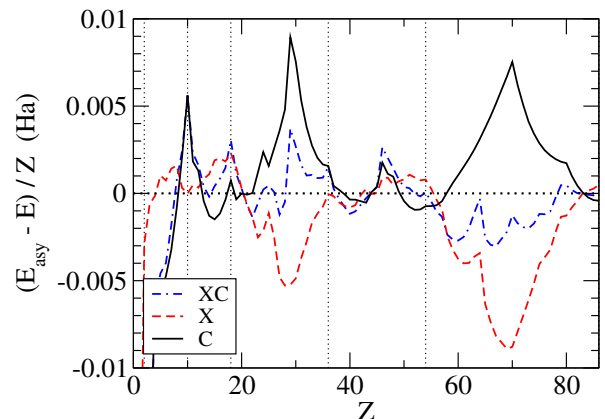


FIG. 10. Difference between the smooth asymptotic limiting functions for asymptotically corrected exchange and correlation energies and their exact values, versus atomic number. XC is exchange-correlation. Vertical lines denote location of noble gases to better visualize the location of periodic table rows.

In Fig 10, we plot the deviations of the exchange and correlation energies per electron from the smooth fits. This is where acRPA is important: To see the periodic pattern in the deviations in the correlation energy by including large  $Z$  values. We have also included vertical lines at the noble gas atoms, to show the periodicity.

There are many interesting features in this plot.

- There is a clear (anti-)correlation between the correlation deviation and the exchange deviation, showing tremendous cancellation of ‘errors’ in the separate components of the deviations. Thus, adding Eqs (70) and  $e_{\text{AC}}^{\text{AE}}(Z)$  yields a much more accurate estimate of XC than either separately. Shell structure is much greater in either exchange or correlation alone than in XC.
- The greatest deviations occur about the middle of the odd rows, and deviations are almost negligible throughout the 4th row.
- We observe the pattern that whenever the most loosely bound electron also has the highest angular

momentum, the deviation grows as that angular momentum subshell is filled, and drops once the next subshell is filled. For example, for  $Z = 21$  to 29, the 3d-shell is being filled and the deviation grows, and then drops rapidly as the 4p's are filled. Note that this only happens when a given subshell is filled for the first time; there is little effect when the 4d's are being filled. A similar pattern appears for the 4f's, and (to a lesser extent) even for the 2p's.

#### IV. CONSEQUENCES

The majority of the numerical work in this manuscript has been devoted to the extraction of an accurate numerical estimate for  $B_C$ , which characterizes the leading correction to LDA correlation for atoms, and is strong evidence for the locality conjecture. In this section, we assume that conjecture is true and discuss its consequences for DFT approximations. We use the mathematical prolog and its relevance to the kinetic energy of non-interacting atoms to illustrate this, by discussing  $T_s[n]$ ,  $E_x[n]$ , and  $E_C[n]$ .

##### A. Relevance of uniform gas to Coulombic matter

In the math prolog, we showed that, for the kinetic energy of non-interacting atoms:

$$T_s(Z) = (3/2)^{1/3} Z^{7/3} - Z^2/2 + \dots \quad (71)$$

For real atoms,

$$T_s(Z) = A_s Z^{7/3} - Z^2/2 + \dots, \quad (72)$$

where  $A_s = 0.768745$  is given exactly by TF theory, while

$$E_x(Z) = -A_x Z^{5/3} + B_x Z + \dots, \quad (73)$$

and

$$E_C(Z) = -A_C Z \ln Z + B_C Z + \dots \quad (74)$$

In every case, a local density approximation yields the leading term for large  $Z$ . Thus, LDA yields the exact large- $Z$  limit of each component for *every* electronic system. It is a *universal* limit for all matter. The form and coefficients of local approximations can be most easily calculated from the uniform electron gas, but in principle can be extracted from taking any system, such as atoms, to the large- $Z$  limit.

But note that correlation is different from exchange and the kinetic energy. In the latter two, the corrections to the dominant term are smaller by a factor of at least  $Z^{-1/3}$ . Thus the corrections are relatively small for  $Z > 50$ , and relatively easily identified. For correlation, the leading term is only  $\ln Z$  larger, meaning  $Z$  must be

vast before it dominates. Thus, lists of values of  $E_C(Z)$  for  $Z < 100$  *alone* cannot be used to extract this behavior accurately. Moreover, approximations (especially any designed only for lighter atoms) can ignore this contribution and still remain accurate. Moreover, since that term is determined by the high-density behavior of the uniform gas, and the next term in LDA is not accurate, all the rest of the correlation energy of the uniform gas is not particularly relevant to atomic correlation energies. Thus almost all popular approximations to  $E_x$  reduce to LDA for uniform densities, but not so for  $E_C$ .

Except for model 1-d systems[14–16, 81, 82], no-one has ever written down a general functional approximation that recovers the leading corrections to LDA for all systems. The gradient expansion approximation does this for slowly-varying densities, but then is quite incorrect for atoms[21]. Generalized gradient approximations attempt to capture both, but find they are irreconcilable[23, 24].

##### B. Performance of semilocal approximations

The locality principle claims that one can understand the successes and failures of semilocal DFT in terms of the large- $Z$  expansion. We now consider three basic properties often calculated with such approximations: ionization potentials, bond energies, and bond lengths. Note that all these depend only on energy differences, not the total energies studied here. But we argue below that the qualitative behavior of semilocal approximations for each of these cases can be understood in terms of the locality principle.

The simplest case is ionization energies, which can be studied for atoms[83]. Within numerical accuracy, at the exchange level, LDA yields the exact ionization energy in the large- $Z$  limit, and GGA (in the PBE case, at least) correctly reduces to LDA in this limit. This is consistent with the fact that GGA's and global hybrids do not typically yield significant improvement over LDA for ionization energies[7, 84]. An analogous result was found for XC: PBE corrections to LDA ionization energies are very small (or zero) in this limit. Thus, at least for atoms, LDA becomes relatively exact for ionization potentials in this limit, and our standard GGA's do not yield much improvement. They do not produce the leading correction in the asymptotic expansion for the ionization potential, and so are not systematically better than LDA for real systems.

Next consider bond energies. GGA's typically improve atomization energies relative to LDA. Both PBE and B88 yield accurate asymptotic corrections to LDA exchange for large  $Z$ . Thus the corrections are accurate for both the equilibrium molecule and the isolated atoms, sufficiently so as to produce improved energy differences. This suggests that both cases are improved by improving the asymptotics.

But now consider what happens as a molecule is stretched relative to equilibrium. The molecular levels

become nearly degenerate. The smaller the gap, the further they are away from the large- $Z$  limit, which assumes a continuum of levels. To see this semiclassically, we note that the Coulson-Fisher point in LDA for  $H_2$  is at  $R = 3.3$  a.u.[85]. If we consider the point where the HOMO level of the exact KS potential just touches the maximum in the KS potential well, this occurs at about the same distance[86]. As  $R$  increases through 3.3, the classical turning point surface of the KS potential at the HOMO energy divides into two isolated regions. Thus the onset of strong static correlation coincides with a qualitative change in the nature of the semiclassical (i.e. local) approximation. The asymptotic expansion works well at equilibrium or for isolated atoms, but fails completely as 3.3 is approached, because of the degeneracy. This is the semiclassical explanation of the failure of semilocal approximations as bonds are stretched.

Finally, we discuss bond lengths, which are determined by the derivative of the binding energy curve at equilibrium. The asymptotic expansion in  $Z$  should work (almost) equally well for separations in and near equilibrium. The classical turning point structure at the HOMO level does not change qualitatively. Furthermore, the asymptotic behavior for large- $Z$  remains the same for each value, and so irrelevant for the derivative. Exchange GGAs that capture the correct asymptotics of the total energy violate the gradient expansion, which should be accurate for these small changes. This was (part of) the

reasoning behind PBESol, which restores the gradient expansion for exchange and improves lattice constants of many solids[22].

### C. Conclusions

The central result of this paper is to combine existing numerical evidence for the correlation energy of non-relativistic atoms to extract the leading correction to the local density approximation for atoms in the large- $Z$  limit. This is a key number that characterizes the leading error made by LDA, and that can be corrected by more sophisticated approximations. We have argued that this number is non-empirical, and should be used as an exact condition for non-empirical construction of functionals. In a preliminary report, we constructed a non-empirical GGA that was asymptotically correct for atoms[87]. The method was then used to impose exact conditions on the SCAN meta-GGA[88].

This work was supported by NSF CHE-1464795. SP was supported by the European Community through the FP7's MC-IIF MODENADYNA, grant agreement No. 623413 and by the European Commission (Grant No. FP7-NMP-CRONOS). TG recognizes computing support from the Griffith University Gowonda HPC Cluster. We thank John Perdew and Raphael Ribeiro for many useful discussions.

- 
- [1] W. Kohn and L. J. Sham, *Phys. Rev.* **140**, A1133 (1965).
  - [2] A. Pribram-Jones, D. A. Gross, and K. Burke, *Annual Review of Physical Chemistry* (2015).
  - [3] F. N. C. Fiolhais and M. Marques, *A Primer in Density Functional Theory* (Springer-Verlag, New York, 2003).
  - [4] A. D. Becke, *Phys. Rev. A* **38**, 3098 (1988).
  - [5] C. Lee, W. Yang, and R. G. Parr, *Phys. Rev. B* **37**, 785 (1988).
  - [6] A. D. Becke, *J. Chem. Phys.* **98**, 5648 (1993).
  - [7] J. P. Perdew, J. A. Chevary, S. H. Vosko, K. A. Jackson, M. R. Pederson, D. J. Singh, and C. Fiolhais, *Phys. Rev. B* **46**, 6671 (1992).
  - [8] J. P. Perdew, K. Burke, and M. Ernzerhof, *Phys. Rev. Lett.* **77**, 3865 (1996), *ibid.* **78**, 1396(E) (1997).
  - [9] S. Kümmel and L. Kronik, *Rev. Mod. Phys.* **80**, 3 (2008).
  - [10] M. Dion, H. Rydberg, E. Schröder, D. C. Langreth, and B. I. Lundqvist, *Phys. Rev. Lett.* **92**, 246401 (2004).
  - [11] M. Levy, *Proceedings of the National Academy of Sciences of the United States of America* **76**, 6062 (1979).
  - [12] E. H. Lieb, *Rev. Mod. Phys.* **53**, 603 (1981).
  - [13] E. H. Lieb and B. Simon, *Advances in Mathematics* **23**, 22 (1977).
  - [14] P. Elliott, D. Lee, A. Cangi, and K. Burke, *Phys. Rev. Lett.* **100**, 256406 (2008).
  - [15] P. Elliott, A. Cangi, S. Pittalis, E. K. U. Gross, and K. Burke, *Phys. Rev. A* **92**, 022513 (2015).
  - [16] R. F. Ribeiro, D. Lee, A. Cangi, P. Elliott, and K. Burke, *Phys. Rev. Lett.* **114**, 050401 (2015).
  - [17] J. Schwinger, *Phys. Rev. A* **22**, 1827 (1980).
  - [18] J. Schwinger, *Phys. Rev. A* **24**, 2353 (1981).
  - [19] J. Conlon, *Communications in Mathematical Physics* **88**, 133 (1983).
  - [20] C. Fefferman and L. Seco, *Advances in Mathematics* **107**, 1 (1994).
  - [21] P. Elliott and K. Burke, *Can. J. Chem.* **87**, 1485 (2009).
  - [22] J. P. Perdew, A. Ruzsinszky, G. I. Csonka, O. A. Vydrov, G. E. Scuseria, L. A. Constantin, X. Zhou, and K. Burke, *Phys. Rev. Lett.* **100**, 136406 (2008).
  - [23] Y. Zhang and W. Yang, *Phys. Rev. Lett.* **80**, 890 (1998).
  - [24] K. B. J.P. Perdew and M. Ernzerhof, *Phys. Rev. Lett.* **80**, 891 (1998).
  - [25] L. A. Constantin, A. Terentjevs, F. Della Sala, P. Cortona, and E. Fabiano, *Phys. Rev. B* **93**, 045126 (2016).
  - [26] S. Laricchia, E. Fabiano, L. A. Constantin, and F. D. Sala, *Journal of Chemical Theory and Computation* **7**, 2439 (2011), pMID: 26606618, <http://dx.doi.org/10.1021/ct200382w>.
  - [27] L. A. Constantin, E. Fabiano, S. Laricchia, and F. Della Sala, *Phys. Rev. Lett.* **106**, 186406 (2011).
  - [28] S. P. McCarthy and A. J. Thakkar, *The Journal of Chemical Physics* **134**, 044102 (2011).
  - [29] H. Kunz and R. Rueedi, *Phys. Rev. A* **81**, 032122 (2010).
  - [30] E. Clementi and G. Corongiu, *International Journal of Quantum Chemistry* **62**, 571 (1997).
  - [31] B.-G. Englert, *Lec. Notes Phys.* **300** (1988).
  - [32] P. Hohenberg and W. Kohn, *Phys. Rev.* **136**, B864 (1964).
  - [33] L. H. Thomas, *Math. Proc. Camb. Phil. Soc.* **23**, 542

- (1927).
- [34] E. Fermi, *Zeitschrift für Physik A Hadrons and Nuclei* **48**, 73 (1928).
- [35] L. Spruch, *Rev. Mod. Phys.* **63**, 151 (1991).
- [36] D. Lee, L. A. Constantin, J. P. Perdew, and K. Burke, *J. Chem. Phys.* **130**, 034107 (2009).
- [37] U. von Barth and L. Hedin, *Journal of Physics C: Solid State Physics* **5**, 1629 (1972).
- [38] D. M. Ceperley and B. J. Alder, *Phys. Rev. Lett.* **45**, 566 (1980).
- [39] S. H. Vosko, L. Wilk, and M. Nusair, *Canadian Journal of Physics* **58**, 1200 (1980), <http://dx.doi.org/10.1139/p80-159>.
- [40] J. P. Perdew and Y. Wang, *Phys. Rev. B* **45**, 13244 (1992).
- [41] R. Jones and O. Gunnarsson, *Rev. Mod. Phys.* **61**, 689 (1989).
- [42] R. O. Jones, *Rev. Mod. Phys.* **87**, 897 (2015).
- [43] R. M. Dreizler and E. K. U. Gross, *Density Functional Theory: An Approach to the Quantum Many-Body Problem* (Springer-Verlag, Berlin, 1990).
- [44] L. Kleinman and S. Lee, *Phys. Rev. B* **37**, 4634 (1988).
- [45] W. H. Miller, *J. Chem. Phys.* **48**, 1651 (1968).
- [46] D. Langreth and J. Perdew, *Phys. Rev. B* **15**, 2884 (1977).
- [47] A. D. Becke, *The Journal of Chemical Physics* **140** (2014), [10.1063/1.4869598](https://doi.org/10.1063/1.4869598).
- [48] E. Engel and R. M. Dreizler, *Density Functional Theory: An Advanced Course* (Springer, Berlin, 2011).
- [49] A. Görling and M. Ernzerhof, *Phys. Rev. A* **51**, 4501 (1995).
- [50] M. Levy and J. Perdew, *Phys. Rev. A* **32**, 2010 (1985).
- [51] J. Harris and R. Jones, *J. Phys. F* **4**, 1170 (1974).
- [52] D. Langreth and J. Perdew, *Solid State Commun.* **17**, 1425 (1975).
- [53] O. Gunnarsson and B. Lundqvist, *Phys. Rev. B* **13**, 4274 (1976).
- [54] E. Lieb and B. Simon, *Phys. Rev. Lett.* **31**, 681 (1973).
- [55] S. Fournais, M. Lewin, and J. P. Solovej, *ArXiv e-prints* (2015), [arXiv:1510.01124 \[math-ph\]](https://arxiv.org/abs/1510.01124).
- [56] J. Scott, *Philos. Mag.* **43**, 859 (1952).
- [57] Z. Levine and P. Soven, *Phys. Rev. Lett.* **50**, 2074 (1983).
- [58] B.-G. Englert and J. Schwinger, *Phys. Rev. A* **26**, 2322 (1982).
- [59] B.-G. Englert and J. Schwinger, *Phys. Rev. A* **29**, 2339 (1984).
- [60] B.-G. Englert and J. Schwinger, *Phys. Rev. A* **29**, 2353 (1984).
- [61] B.-G. Englert and J. Schwinger, *Phys. Rev. A* **29**, 2331 (1984).
- [62] B.-G. Englert and J. Schwinger, *Phys. Rev. A* **32**, 26 (1985).
- [63] B.-G. Englert and J. Schwinger, *Phys. Rev. A* **32**, 36 (1985).
- [64] B.-G. Englert and J. Schwinger, *Phys. Rev. A* **32**, 47 (1985).
- [65] K. Burke, M. Ernzerhof, and J. P. Perdew, *Chemical Physics Letters* **265**, 115 (1997).
- [66] J. P. Perdew, L. A. Constantin, E. Sagvolden, and K. Burke, *Phys. Rev. Lett.* **97**, 223002 (2006).
- [67] S. P. McCarthy and A. J. Thakkar, *The Journal of Chemical Physics* **136**, 054107 (2012).
- [68] S. J. Chakravorty, S. R. Gwaltney, E. R. Davidson, F. A. Parpia, and C. F. Fischer, *Phys. Rev. A* **47**, 3649 (1993).
- [69] H. Eshuis, J. Bates, and F. Furche, *Theoretical Chemistry Accounts* **131**, 1 (2012).
- [70] S. Lebègue, J. Harl, T. Gould, J. G. Ángyán, G. Kresse, and J. F. Dobson, *Phys. Rev. Lett.* **105**, 196401 (2010).
- [71] T. Björkman, A. Gulans, A. V. Krasheninnikov, and R. M. Nieminen, *Journal of Physics: Condensed Matter* **24**, 424218 (2012).
- [72] T. Gould and J. F. Dobson, *The Journal of Chemical Physics* **138**, 014103 (2013).
- [73] T. Gould and J. F. Dobson, *The Journal of Chemical Physics* **138**, 014109 (2013).
- [74] T. Gould and J. Toulouse, *Phys. Rev. A* **90**, 050502 (2014).
- [75] S. Chakravorty and E. Davidson, *J. Phys. Chem.* **100**, 6167 (1996).
- [76] M. Gell-Mann and K. Brueckner, *Phys. Rev.* **106**, 364 (1957).
- [77] L. Onsager, L. Mittag, and M. J. Stephen, *Ann. Phys. (Leipzig)* **18** (1966).
- [78] J. E. Bates and F. Furche, *The Journal of Chemical Physics* **139**, 171103 (2013), <http://dx.doi.org/10.1063/1.4827254>.
- [79] S. Kurth and J. P. Perdew, *Phys. Rev. B* **59**, 10461 (1999).
- [80] Z. Yan, J. P. Perdew, S. Kurth, C. Fiolhais, and L. Almeida, *Phys. Rev. B* **61**, 2595 (2000).
- [81] A. Cangi, D. Lee, P. Elliott, and K. Burke, *Phys. Rev. B* **81**, 235128 (2010).
- [82] A. Cangi, D. Lee, P. Elliott, K. Burke, and E. K. U. Gross, *Phys. Rev. Lett.* **106**, 236404 (2011).
- [83] L. A. Constantin, J. C. Snyder, J. P. Perdew, and K. Burke, *The Journal of Chemical Physics* **133**, 241103 (2010).
- [84] G. I. Csonka, J. P. Perdew, and A. Ruzsinszky, *Journal of Chemical Theory and Computation* **6**, 3688 (2010), <http://dx.doi.org/10.1021/ct100488v>.
- [85] R. A. R. Bauernschmitt, *Chem. Phys. Lett.* **256**, 454 (1996).
- [86] M. A. Buijse, E. J. Baerends, and J. G. Snijders, *Phys. Rev. A* **40**, 4190 (1989).
- [87] K. Burke, A. Cancio, T. Gould, and S. Pittalis, *submitted and arXiv:1409.4834v1* (2014).
- [88] J. Sun, A. Ruzsinszky, and J. P. Perdew, *Phys. Rev. Lett.* **115**, 036402 (2015).